JOURNAL OF GEOPHYSICAL RESEARCH, VOL. 107, NO. D24, 4760, doi:10.1029/2001JD001259, 2002

Drag coefficient and plant form response to wind speed in three plant species: Burning Bush (*Euonymus alatus*), Colorado Blue Spruce (*Picea pungens* glauca.), and Fountain Grass (*Pennisetum setaceum*)

J. A. Gillies
Division of Atmospheric Sciences, Desert Research Institute, Reno, Nevada, USA

W. G. Nickling and J. King
Department of Geography, University of Guelph, Guelph, Ontario, Canada

Received 28 August 2001; revised 28 February 2002; accepted 13 March 2002; published 19 December 2002.

[1] Whole-plant drag coefficients (C_d) for three plant species: Burning Bush (*Euonymus alatus*), Colorado Blue Spruce (*Picea pungens* glauca.), and Fountain Grass (*Pennisetum setaceum*) in five different porosity configurations were developed from force versus wind speed data collected with a force balance in a recirculating wind tunnel. The average C_d for the Burning Bush, Colorado Spruce, and Fountain Grass in their untrimmed forms were 0.42 (±0.03), 0.39 (±0.04), and 0.34 (±0.06), respectively. Drag curves (C_d versus flow Reynolds number (R_e) function) for the Burning Bush and Colorado Spruce were found to exhibit, for the lower porosity configurations, a rise to a maximum around flow Reynolds numbers ($R_e = \rho u_h h/\nu$) of 2×10^5. Fountain Grass C_d was shown to be dependent upon R_e to values $>5 \times 10^5$. The Burning Bush and Colorado Spruce plants reduced their drag, upon reaching their maxima, by decreasing their frontal area and increasing their porosity. Maximum C_d for these plants occurred at optical porosities of ~0.20. The Fountain Grass reduced drag at high R_e by decreasing frontal area and porosity. The mechanism of drag reduction in Fountain Grass was continual reconfiguration to a more aerodynamic form as evidenced by continual reduction of C_d with R_e. *INDEX TERMS:* 3322 Meteorology and Atmospheric Dynamics: Land/atmosphere interactions; 3307 Meteorology and Atmospheric Dynamics: Boundary layer processes; 3399 Meteorology and Atmospheric Dynamics: General or miscellaneous; 0315 Atmospheric Composition and Structure: Biosphere/atmosphere interactions; *KEYWORDS:* drag coefficients, vegetation, porosity

Citation: Gillies, J. A., W. G. Nickling, and J. King, Drag coefficient and plant form response to wind speed in three plant species: Burning Bush (*Euonymus alatus*), Colorado Blue Spruce (*Picea pungens* glauca.), and Fountain Grass (*Pennisetum setaceum*), *J. Geophys. Res.*, *107*(D24), 4760, doi:10.1029/2001JD001259, 2002.

1. Introduction

[2] Understanding the drag force generated on plants is important for assessing their influence on boundary layer flow and exchange processes of momentum and scalar atmospheric constituents such as heat, water vapor, or CO_2, as well as particulate matter. This applies to both a horizontally uniform or continuous plant canopy [*Raupach*, 1987; *Massman and Weil*, 1999] as well as for discontinuous or sparse covers.

[3] *Raupach* [1992] proposed a physically based model, which evaluates the partitioning of wind shear in the context of solid elements with well-defined wakes. An important input parameter in the model is the drag coefficient of the surface roughness elements such as vegetation, which is normally assigned a value based on a solid element of similar shape. Recent research, however [*Gillies et al.*, 2000; *Grant and Nickling*, 1998; *Wyatt and Nickling*, 1997], suggests that vegetation, because of its complex internal and external geometry and flexibility, has drag coefficients considerably higher than solid elements of similar size and shape.

[4] Knowledge of a plant's ability to absorb momentum from the wind can also be used for practical purposes in designing efficient control strategies to reduce wind erosion and dust emissions with vegetation [*Gillies et al.*, 2000] using shear stress partitioning relationships [*Wolfe and Nickling*, 1996; *Wyatt and Nickling*, 1997]. Plants offer a measure of protection from erosive winds to the bare intervening surface by decreasing the available shear force through processes of momentum extraction.

[5] Vegetation has greater potential to absorb momentum compared to solid elements because of their porous and flexible nature. Flexibility in the stems and branches as well as the mobility of leaves allows energy to dissipate through bending and swaying and fluttering of leaves or needles. The increased momentum absorption occurs through the

Copyright 2002 by the American Geophysical Union.
0148-0227/02/2001JD001259

wind-form interaction. The dissipation of momentum may also occur through the development of turbulent structures within the plants or eddy shedding in their lee.

[6] The drag coefficient (C_d) for an isolated solid element can be described by

$$C_d = \frac{F}{\rho A_t u_z^2}, \quad (1)$$

where F is total force on the element (N), ρ is air density (kg m^{-3}), A_t is element cross sectional area (m^2), and u_z is wind speed (m s^{-1}) at height z (m). Two types of drag are associated with vegetation, form drag and viscous drag. The amount of viscous drag depends on the characteristics of the plant's leaf and stem components. For example, fine-leafed vegetation like grasses is likely to have higher viscous drag than broad leaf plants.

[7] Drag coefficients for solid elements plotted as a function of flow Reynolds number (R_e) typically show an initial rapid decline followed by a leveling off to a relatively constant level at higher R_e values [*Taylor*, 1988]. Pure viscous drag is approximately proportional to $R_e^{-0.5}$. R_e is defined here as

$$R_e = \frac{\rho u_h h}{\nu}, \quad (2)$$

where u_h is the horizontal and time average wind speed (m s^{-1}) over the layer from the height of the lowest measurement (0.053 m above the surface) to the plant height h (m), and ν is kinematic viscosity of air (m^2 s^{-1}).

[8] *Grant and Nickling* [1998] and *Gillies et al.* [2000] demonstrated that the C_d for porous and flexible vegetation was greater than solid element forms of the same physical dimensions. *Grant and Nickling* [1998] estimated a C_d of 0.4 for an artificial tree and *Gillies et al.* [2000] reported average C_d values of ~1.4 and ~0.49 for a small (0.6 m high, 0.5 m wide) and larger (1.6 m high and 1.3 m wide) desert shrub (Greasewood, *Sarcobatus vermiculatis*), respectively. *Wyatt* [1996] estimated the C_d for a creosote bush (*Larrea tridenta*) at ~0.49. *Gillies et al.* [2000] also reported that the C_d for Greasewood, unlike a solid element, did not reach an equilibrium value for R_e up to 6×10^5, but continued to slowly decline as a power function of R_e, indicating that these shrubs extract momentum less effectively as wind speeds increase. However, they assumed the frontal area and the porosity of Greasewood were constant over the wind speeds and R_e range their shrubs were exposed to. If the frontal area and porosity of the Greasewood had changed proportionally as wind speed increased the C_d may have reached an equilibrium value. *Gillies et al.* [2000] did not have the means to assess incremental changes in plant frontal area and porosity as a function of changing wind speed. However, they did note that the condition of the Greasewood they tested was very stiff and likely deformed little in response to increased wind speed.

[9] Plants will likely reach a final form in response to the aerodynamic forces acting upon them. Whether they can maintain this form without a loss of leaves or failure in the stems, branches, and trunk is probably species and in the case of trees age dependent as well [*Ennos*, 1999]. The purpose of this paper is to examine plant form response to increasing wind speed and present whole-plant drag coefficients from direct measurements of wind force on three different plant species chosen to represent three different basic plant designs. The three plants tested were a small leafy shrub (Burning Bush, *Euonymus alatus*), a small coniferous tree (Colorado Blue Spruce, *Picea Pungens* glauca.), and an ornamental grass (Fountain Grass, *Pennisetum setaceum*). They should not be considered as being the definitive form of their species, but representative of a morphological type. Addressing intraplant variability was not an objective of this study. Drag curves and drag coefficients for the different plants were estimated from the collected force and wind speed data. The force on the plants was measured with a force balance. The plants were tested in a wind tunnel in their original form and then were systematically pruned four times to alter the number of leaves for the Burning Bush (BB), branches for the Colorado Spruce (CS), and blades for the grass plant (FG). By simultaneously measuring the wind speed, drag force on the plants, and plant frontal area and optical porosity, the effects of the latter two characteristics on the calculated plant C_d were also evaluated.

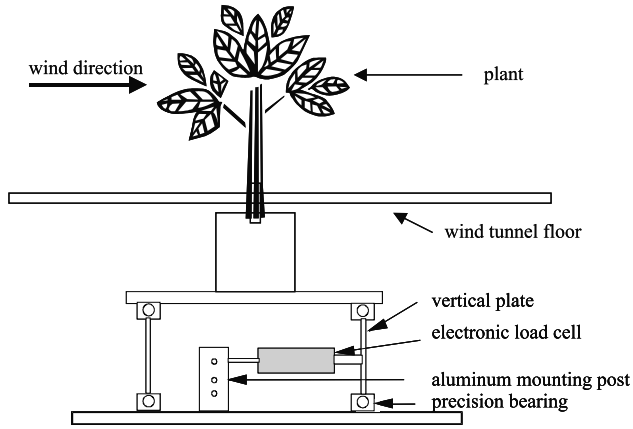

Figure 1. Schematic diagram of the force balance.

2. Experimental Design

2.1. Element Drag

[10] The drag force generated on the plants was measured directly with a force balance on which the plants were mounted. A schematic diagram of the force balance is shown in Figure 1.

[11] The force balance was set below the floor of the University of Guelph's recirculating wind tunnel. The force on the plant was recorded by reading the load cell in the force balance at 1 Hz with a PC via serial communication. The wind tunnel is a recirculating design with a 9 m long working section 1 m wide and 1 m high. Wind speed in the tunnel is measured with a Pitot tube rake consisting of six individual tubes spaced logarithmically with height (0.053, 0.095, 0.153, 0.203, 0.277, and 0.355 m) connected to a scanning valve and a pressure transducer linked to an analog to digital board in the same PC recording the load cell in the force balance. Wind speeds are recorded at 1 Hz for each tube. Typically, 10 to 20 scans of the entire Pitot tube rake were made to estimate the average wind speed in the tunnel at a specific wind speed setting. Wind speed in

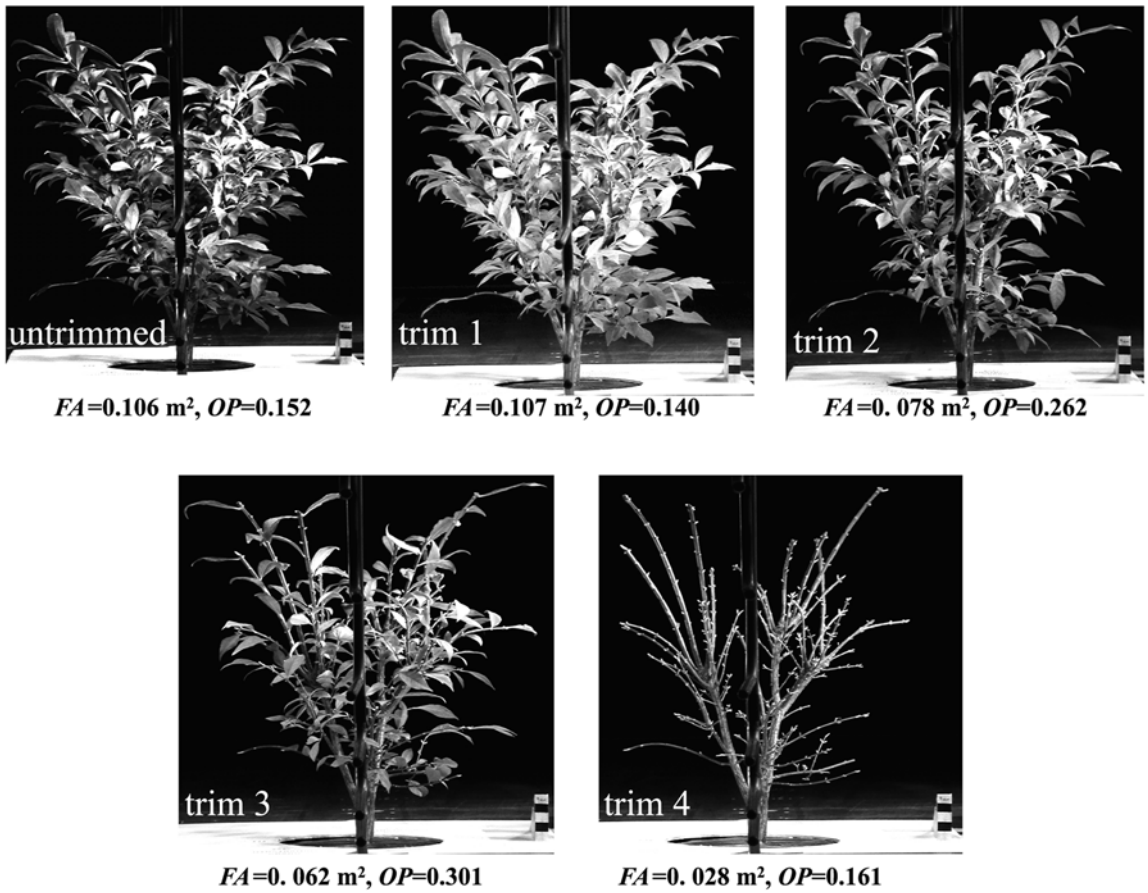

Figure 2. The pruning sequence (trim condition) for the Burning Bush. The frontal area (FA) and optical porosity (OP) for each trim condition in still air conditions are shown for comparison purposes.

the tunnel is regulated with a computer controlled, variable speed DC motor. Each plant and porosity configuration was subjected to seven different average wind speeds (nominally 1.5, 3.0, 5.0, 6.5, 8.5, 10, and 12.0 m s^{-1}) measured at a height of 0.355 m above the wind tunnel floor. Upon completion of the measurement of the wind speed profile and force on the plant at each increment the velocity in the tunnel was increased and allowed to come to equilibrium for 60 s prior to the next measurements.

2.2. Vegetation Characterization

[12] The plants used in this experiment were chosen to reflect three basic plant designs. The BB represents a small deciduous shrub with finely toothed leaves on opposite sides of the stems. A front-on view approximates an ellipsoid (egg shape) with the narrow end pointing down. The CS represents a young coniferous tree. In the CS the needles are spread around the stem, with more located above the stem than below. They are four sided and stiff and rigid. A front-on view approximates a triangle and in three dimensions a cone. The FG typifies grasses that grow in clumps or tussocks separated from each other by open areas. Its configuration in this experiment approximated a hemispherical shape in still air conditions.

[13] Each plant was first tested in the condition it was received from the nursery. Following the initial testing in the wind tunnel the plants were modified by removing parts from them. Each plant was pruned four times and the force versus wind speed measurements taken after each successive pruning. As each plant had a different basic form, a different pruning strategy was used for each. For the BB, the leaves were removed systematically by plucking every other leaf on a stem, while trying to preserve the basic pinnate leaf pattern (Figure 2). The CS was pruned by removing individual branches, as removing needles was deemed logistically unfeasible. For each pruning the smallest needle-covered branches were removed from the main branches radiating from the central trunk (Figure 3). To prune the FG, blades were cut from the base of the clump taking care to remove a range of blade lengths so as to keep the same nominal height and width of the clump but to increase its porosity (Figure 4).

[14] Within the tunnel the plants were illuminated by Halogen flood lamps shining through the roof and Plexiglas side of the tunnel. In addition, a large mirror was placed on the wall of the wind tunnel opposite the Plexiglas side to add illumination and avoid shadowed zones in the plant. A digital camera was placed ~2.5 m upwind of the plant in the centerline of the wind tunnel. The camera recorded still-frame digital images of the plants in the wind tunnel while they were subjected to the different wind speeds. A milled aluminum block of known dimensions was placed beside the plant, which provided a scale to reference the size of the object in the acquired images.

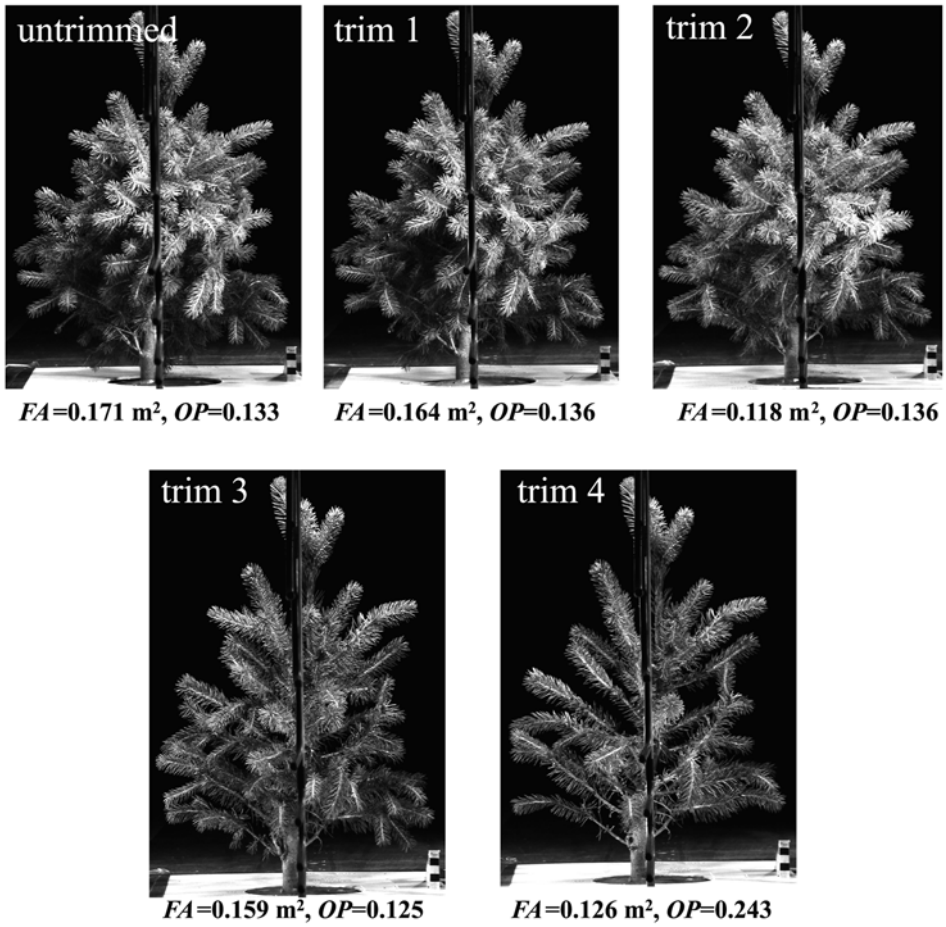

Figure 3. The pruning sequence (trim condition) for the Colorado Spruce. The frontal area (FA) and optical porosity (OP) for each trim condition in still air conditions are shown for comparison purposes.

[15] The digital images were used to estimate the frontal area (FA) and optical porosity (OP) of the plants. The images of the plants were analyzed using IDRISI software (Clark Labs, Worcester, Mississippi). The FA was estimated by counting the number of pixels within a stated range of gray color and applying the scaling relationship between pixel size and length as determined from having the aluminum block in the digital image, which provided a reference scale.

[16] Estimating OP for the plants required some degree of subjectivity. The difficulty lies in defining what a pore, which has three dimensions, looks like in the two dimensions of the digital image. The part of the plant that is the most difficult to define pores for is the outer edge. In addition, the three plants that were chosen for study present different challenges for defining pores due to their morphologies. To minimize the bias in defining pores several simple rules were followed. These were as follows: (1) Any part of the plant that allowed light to pass through the plant to form a closed object constituted a pore, and (2) near the plant edges a pore was designated as such if the gap between the two closest leaves (or branches) was less than a quarter of the total width of the partially leaf-enclosed area (Figure 5). Type 1 pores were the majority for all three plants. Rule 2 was easily applied for the BB and FG plants. However, to define edge pores for the CS a different methodology was used. For the CS images a vector polygon was mapped on top of the raster data and a polygon created by outlining the entire CS image by connecting the needle ends point-to-point. The area between two joined needles was defined as a pore. Essentially a zone of influence of wind and plant interaction around the perimeter was defined with the assumption being that this zone acted similarly to an enclosed pore in the interior of the plant.

[17] The OP was calculated through the use of calibrated raster cell area by

$$\mathrm{OP} = \frac{(\text{total pore area})}{(\text{total solid plant area}) + (\text{total pore area})} \tag{3}$$

The area of individual raster cells was calculated using the scale included in each photograph. To minimize the bias in defining pores using the above rules and methods the same person analyzed all the images.

[18] It should be recognized that two-dimensional OP is a surrogate measure of the three-dimensional porosity of these plants. The actual pathways that air can take to pass

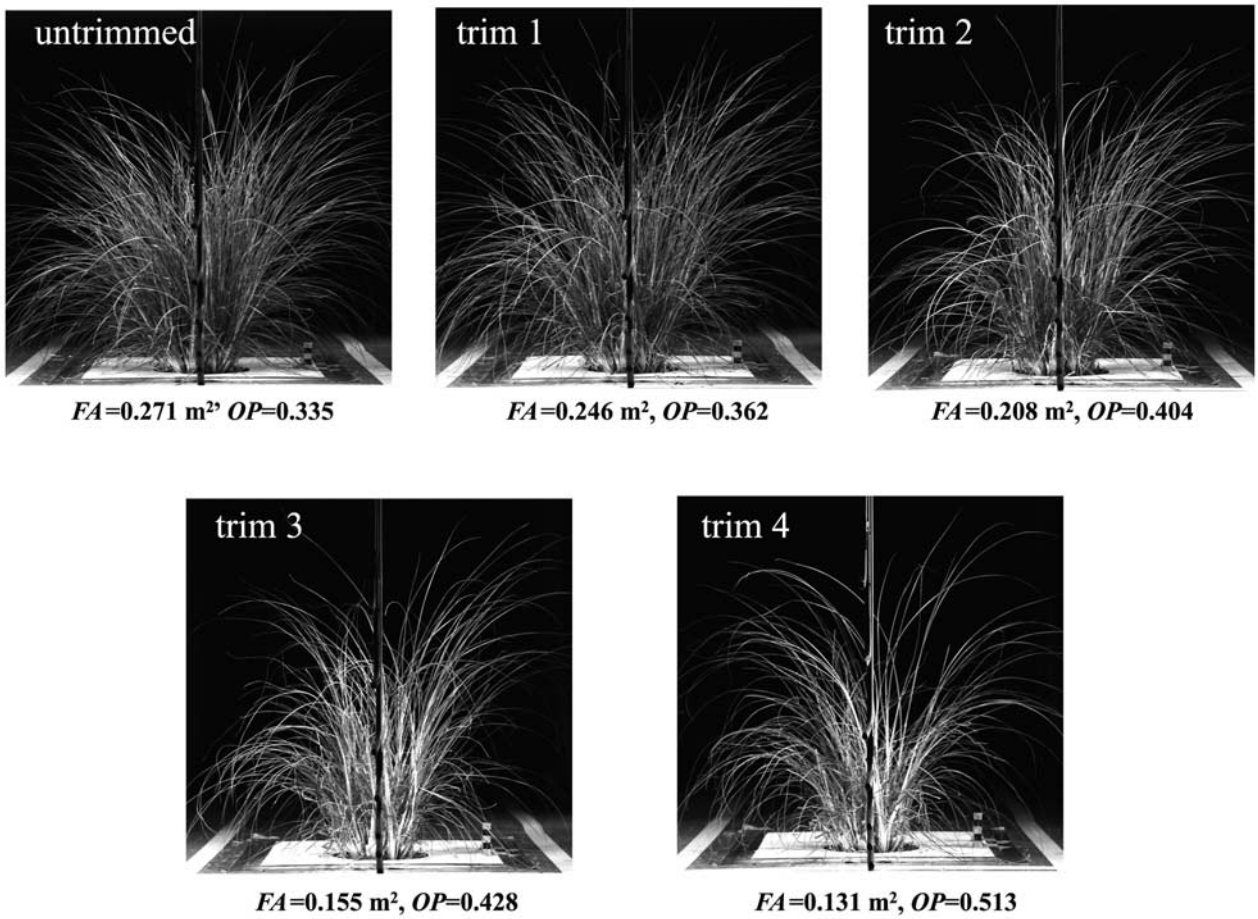

Figure 4. The pruning sequence (trim condition) for the Fountain Grass. The frontal area (FA) and optical porosity (OP) for each trim condition in still air conditions are shown for comparison purposes.

through a plant are not the same as for a light ray that can only travel in a straight line. This is a potential shortcoming of the OP measurement, as it does not effectively capture the true effect of porosity on the airflow. However, it is commonly used and is a relatively easy measure to acquire for characterizing plant structure. *Grant and Nickling* [1998] demonstrated a strong relationship between OP and the volumetric porosity of artificial vegetation.

3. Results

3.1. Plant Drag Coefficients

[19] The laboratory measurements indicated strong relationships between the force on the plants measured with the force balance and the square of average wind speed measured over the height of the plant. The force versus wind speed squared data was linear for the CS plant in each trim condition. However, for the FG in all cases and the BB for the no trim through trim 3 conditions the relationship was better described by a power function. Examples of this relationship for each of the three plants for their un-pruned conditions are shown in Figure 6. A total of 15 separate curves relating force on the plants to wind speed squared were generated for the three plants (Table 1).

[20] On the basis of the force and wind speed squared data as well as the frontal area estimates from the digital image analysis, C_d for each wind speed and porosity configuration were calculated using equation (1). Examples of the C_d for the different plant species plotted as a function of R_e for the untrimmed condition are shown in Figure 7.

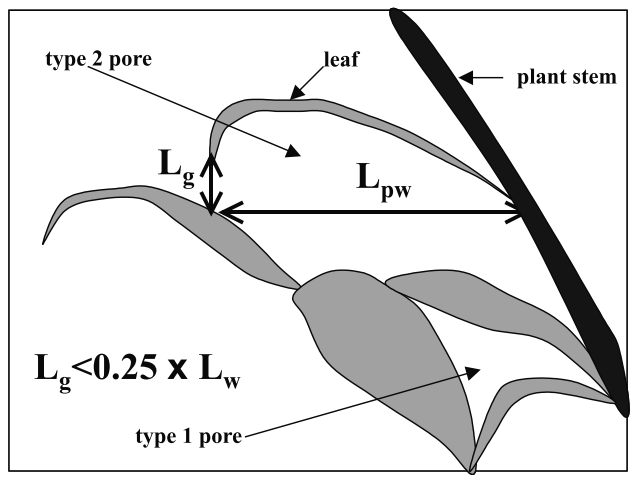

Figure 5. A plant edge pore (type 2), defined as such if the length of the gap (L_g) between two close leaves is less than one quarter the length of the distance across the open area (L_{pw}) where an intersection would occur. A type 1 pore is also identified.

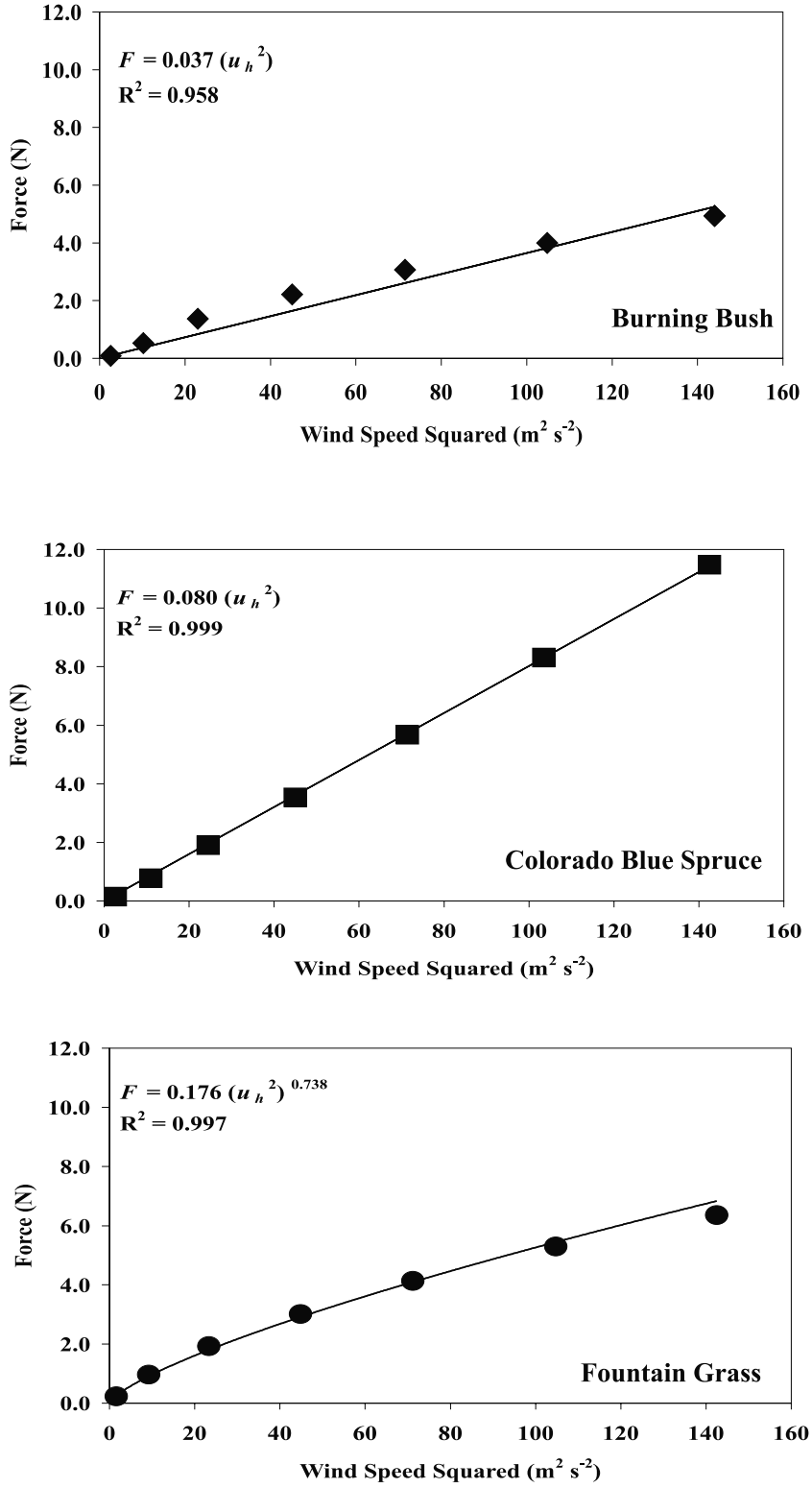

Figure 6. Examples of the force versus wind speed squared relationships for each of the three plant species in their untrimmed condition. The subscript on the wind term u in the force equations denotes the average wind speed over the height of the plant.

The calculated C_d values for each plant type for each trim condition are listed in Table 2. The BB and CS can have quite different drag curve forms than has been observed for solid elements and other plants species such as Greasewood as presented by *Gillies et al.* [2000]. For the BB plant in all trim conditions, there is an initial increase in C_d as a function of R_e to a maximum and then a decline to a relatively stable value. This same increase of C_d with R_e

Table 1. Force Versus Wind Speed Squared Relationships for Each Plant and Each Trim Condition

	Burning Bush[a]		Colorado Spruce		Fountain Grass[b]	
Trim Condition	$F(N) = a\ (u_h^2)$	R^2	$F\ (N) = a\ (u_h^2)$	R^2	$F\ (N) = a\ (u_h^2)^b$	R^2
Untrimmed	$F = 0.037\ (u_h^2)$	0.958	$F = 0.080\ u_h^2$	0.999	$F\ (N) = 0.176\ (u_h^2)^{0.738}$	0.997
	$F\ (N) = 0.046\ (u_h^2)^{0.976}$	0.976				
Trim 1	$F = 0.034\ (u_h^2)$	0.959	$F = 0.077\ u_h^2$	0.999	$F\ (N) = 0.165\ (u_h^2)^{0.713}$	0.997
	$F\ (N) = 0.051\ (u_h^2)^{0.931}$	0.985				
Trim 2	$F = 0.030\ (u_h^2)$	0.984	$F = 0.075\ u_h^2$	0.999	$F\ (N) = 0.091\ (u_h^2)^{0.775}$	0.995
	$F\ (N) = 0.038\ (u_h^2)^{0.962}$	0.989				
Trim 3	$F = 0.023\ (u_h^2)$	0.987	$F = 0.062\ u_h^2$	0.999	$F\ (N) = 0.072\ (u_h^2)^{0.750}$	0.998
	$F\ (N) = 0.027\ (u_h^2)^{0.976}$	0.997				
Trim 4	$F = 0.010\ (u_h^2)$	0.999	$F = 0.049\ u_h^2$	0.999	$F\ (N) = 0.500\ (u_h^2)^{0.762}$	0.995
	$F\ (N) = 0.008\ (u_h^2)^{1.052}$	0.999				

[a] Slope value a estimated from linear least squares regression analysis of the force versus wind speed squared relationship using a zero-force on the intercept.
[b] Coefficients a and b estimated from nonlinear least squares regression analysis of the force versus wind speed squared relationship.

is observed for the untrimmed through trim 2 case for the CS. In the CS trim 3 case, C_d initially declines and then appears to level off, and for trim 4 there is a relatively constant C_d over the measured R_e range. The drag curves for the FG follow the more typical pattern associated with solid elements that show an initial steep decline followed by a leveling off to relatively constant level. However, the FG curves are similar to several of the Greasewood curves of *Gillies et al.* [2000] as they show a dependence on R_e, at least to the limits of the range tested ($\sim 5 \times 10^5$).

3.2. Plant Frontal Areas and Optical Porosities

[21] The FA and OP of each plant configuration and its associated wind speed condition are listed in Table 2. The BB and CS plants can initially respond to a low wind condition by decreasing their frontal area with respect to its still air value (Table 2). With increasing wind speed (and R_e) the BB and CS plants present more FA to the wind and often increase their FA to values greater than the still air condition (Table 2). The tendency of the leaves to align themselves with their maximum projected area perpendicular to the airflow at low to moderate wind speeds is a well-known flow form phenomenon [*Middleton and Southard*, 1984]. With increasing wind speed a threshold is reached where these two plant types begin to decrease their FA as the force of the wind causes them to deform into a shape that presents less FA. To compare the effect of increasing wind speed on FA for each plant species and level of pruning, the FA was normalized to the still air value for each trim condition. The relationships between wind speed and normalized FA (NFA) for the BB and CS plants are shown in Figure 8. The effect of increasing NFA with increasing wind speed followed by a decline past a threshold wind speed value is shown most clearly by the BB in the series of images presented in Figure 9 for the untrimmed condition. The same effect is observed in the CS, but it is subtler. In the final trim condition for the BB (i.e., no leaves) the NFA of the BB was essentially constant with wind speed (Figure 8).

[22] The FG responds differently than the BB and CS showing a continual decrease in NFA as wind speed increases (Figure 10). The continual decrease in NFA likely reflects the morphology of the grass stalks which are somewhat cylindrical and thus have no preferred orientation into the wind stream. This is unlike thin flat forms such as leaves that tend to align themselves perpendicular to the air stream. The NFA behavior for FG is also likely to reflect the lower rigidity and greater deformability with increasing wind speed of a grass (FG) relative to a woody plant (BB and CS). The decrease in NFA for the FG follows an exponential function over the range of wind speeds tested (Figure 10a). For all the relationships shown in Figures 8 and 10, the same form of the response curves of NFA is observed if force is used in place of wind speed. The NFA response shows slightly better fit to the wind speed rather than the force data, which have slightly greater associated uncertainties.

[23] Plant OP appears to have a complex response to wind speed similar to the FA response for the BB and CS plants and a simpler predictable behavior for the FG that matches the behavior of FA in the FG. To compare and contrast the form response between plants and across the five trim conditions the relationship between normalized OP (NOP) and average wind speed were plotted along with NFA in Figure 8. The still air OP value was used in the normalization procedure.

[24] Comparing the BB and CS NFA and NOP data for the range of wind speeds tested suggests that these two parameters often show a negative correlation. Plots of the relationship between NFA and NOP for the BB and CS plants are presented in Figure 11. This negative correlation was observed to occur more frequently for the CS plant (four out of five trim conditions) and for a wider range of wind speeds than for the BB plant where it was observed to more likely occur when wind speeds were less than 7 m s^{-1} (Figure 11). In these cases it appears that as the plants present less NFA more straight through pathways open up and NOP increases; conversely, as NFA increases, there is a reduction in these pathways and NOP declines.

[25] The NOP response to increasing wind speed in the FG shows an exponential decline over the range of wind speeds tested (Figure 10). This mirrors the response of NFA to increasing wind speed (Figure 10), and there is a strong positive linear relationship between NOP and NFA over the range of conditions tested (Figure 12), unlike the other two plants tested. For the FG, as wind speed increases, the FA declines simultaneously with OP, and the plant becomes smaller and less porous even as C_d declines.

4. Discussion

4.1. Force Versus Wind Speed Relationships

[26] Investigations into the aerodynamic characteristics of trees to evaluate whether they reduce drag by reconfi-

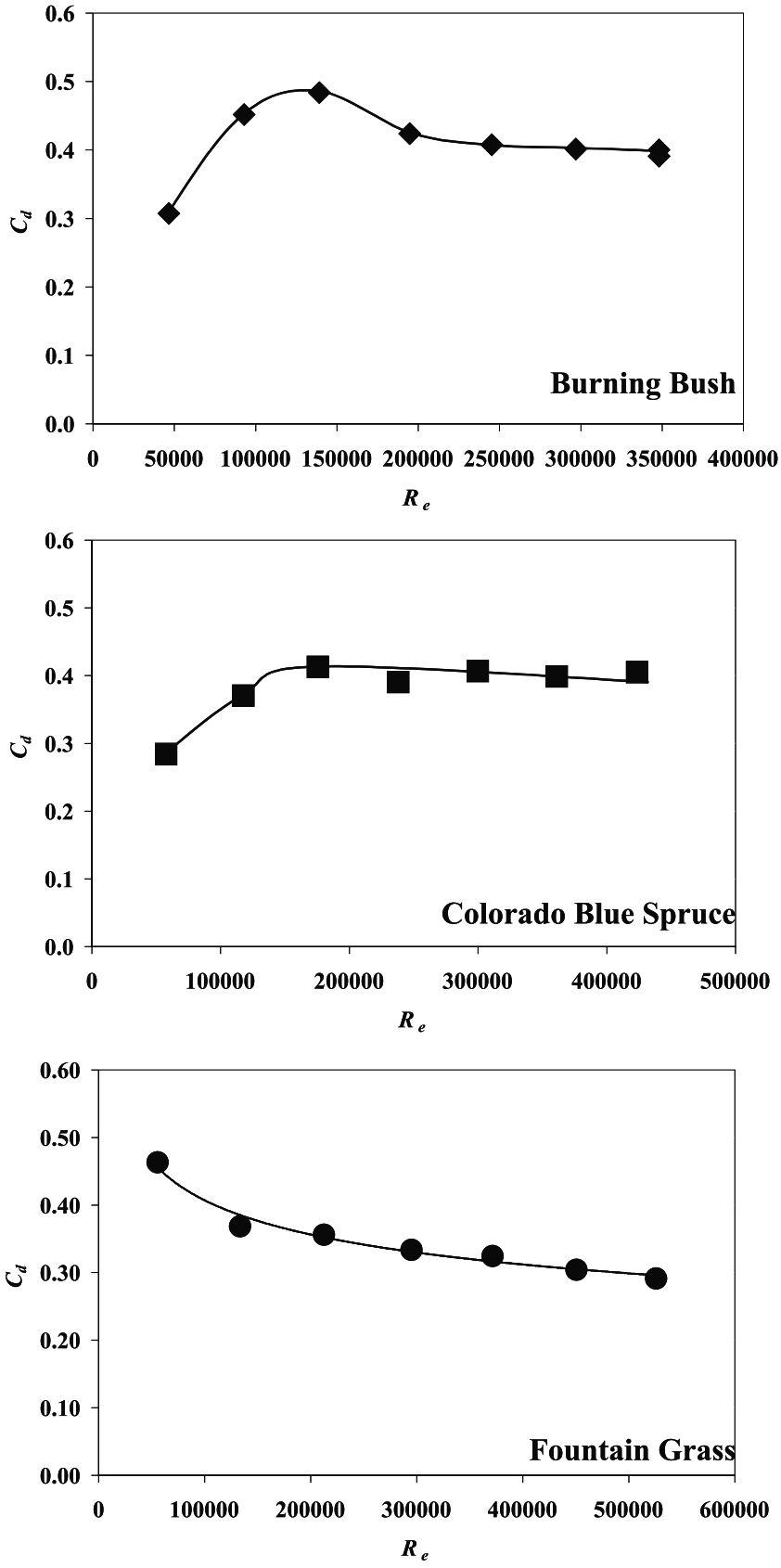

Figure 7. Drag curves developed from the force versus wind speed squared data shown in Figure 6.

Table 2. Summary of Plant Characteristics and Calculated Drag Coefficients for the Three Plants for Each Trim Condition

	Burning Bush				Colorado Spruce				Fountain Grass			
Trim Condition	OP[a]	FA[b], m^2	R_e	C_d	OP	FA, m^2	R_e	C_d	OP	FA, m^2	R_e	C_d
untrimmed	0.152	0.106	0	N/A[c]	0.133	0.171	0	N/A	0.335	0.271	0	N/A
	0.230	0.089	46662	0.31	0.120	0.170	57525	0.28	0.320	0.263	55480	0.46
	0.216	0.095	92925	0.45	0.127	0.172	117707	0.37	0.198	0.241	133398	0.37
	0.176	0.104	139127	0.48	0.135	0.170	175517	0.41	0.241	0.195	212528	0.36
	0.155	0.098	194753	0.42	0.130	0.170	237876	0.39	0.225	0.170	294880	0.33
	0.163	0.089	245296	0.41	0.141	0.165	299845	0.41	0.206	0.151	371518	0.32
	0.180	0.080	296989	0.40	0.120	0.168	360987	0.40	0.194	0.140	450594	0.30
	0.139	0.074	348103	0.39	0.108	0.166	423573	0.41	0.179	0.129	525687	0.29
	0.139	0.072	348103	0.40	0.108	0.164	423573	0.41	0.179	0.124	525687	0.30
trim 1	0.140	0.107	0	N/A	0.136	0.164	0	N/A	0.362	0.246	0	N/A
	0.173	0.099	43576	0.33	0.114	0.167	49049	0.30	0.361	0.235	51361	0.47
	0.156	0.102	91694	0.41	0.149	0.163	111224	0.38	0.287	0.201	122586	0.38
	0.157	0.108	142453	0.41	0.115	0.171	172862	0.37	0.242	0.178	184302	0.36
	0.148	0.108	192579	0.36	0.158	0.165	235420	0.40	0.155	0.156	253071	0.32
	0.143	0.101	244472	0.33	0.168	0.161	298190	0.41	0.187	0.139	327010	0.30
	0.131	0.087	297097	0.34	0.162	0.159	359068	0.40	0.140	0.126	398439	0.28
	0.171	0.075	348892	0.36	0.148	0.156	420612	0.40	0.136	0.116	471282	0.26
	0.171	0.070	348892	0.38	0.148	0.158	420612	0.40	0.136	0.107	471282	0.28
trim 2	0.262	0.078	0	N/A	0.118	0.165	0	N/A	0.404	0.208	0	N/A
	0.240	0.078	39698	0.32	0.140	0.163	60554	0.26	0.360	0.193	58832	0.29
	0.205	0.086	85221	0.39	0.154	0.161	114109	0.38	0.272	0.164	124249	0.30
	0.186	0.089	133579	0.40	0.124	0.165	173922	0.39	0.280	0.135	190489	0.30
	0.217	0.078	182292	0.39	0.119	0.170	235775	0.38	0.238	0.122	258781	0.28
	0.184	0.072	229661	0.38	0.156	0.160	297497	0.40	0.146	0.115	328564	0.25
	0.182	0.066	279653	0.38	0.125	0.159	356948	0.40	0.146	0.099	396333	0.26
	0.190	0.069	325140	0.35	0.168	0.152	420377	0.41	0.185	0.091	449496	0.26
	0.190	0.064	325140	0.38	0.168	0.151	420377	0.42	0.185	0.091	449496	0.26
Trim 3	0.301	0.062	0	N/A	0.222	0.143	0	N/A	0.428	0.155	0	N/A
	0.276	0.065	35938	0.32	0.229	0.143	41254	0.55	0.459	0.145	48694	0.33
	0.235	0.067	85629	0.33	0.222	0.144	109309	0.39	0.346	0.128	112932	0.28
	0.194	0.068	132241	0.34	0.234	0.143	173363	0.39	0.315	0.110	176264	0.26
	0.228	0.063	177786	0.34	0.232	0.142	235230	0.39	0.230	0.098	239263	0.25
	0.176	0.063	225889	0.33	0.228	0.140	297871	0.39	0.256	0.090	303602	0.23
	0.239	0.060	273271	0.33	0.252	0.135	362027	0.39	0.146	0.085	365250	0.21
	0.152	0.060	324989	0.30	0.188	0.138	432738	0.37	0.115	0.075	420215	0.22
	0.152	0.057	324989	0.31	0.188	0.137	432738	0.38	0.115	0.073	420215	0.23
Trim 4	0.166	0.028	0	N/A	0.243	0.126	0	N/A	0.513	0.131	0	N/A
	0.187	0.028	38302	0.25	0.239	0.125	46664	0.38	0.511	0.118	45065	0.26
	0.182	0.028	83706	0.29	0.263	0.122	106661	0.38	0.377	0.102	94960	0.26
	0.181	0.028	129604	0.30	0.245	0.126	171156	0.35	0.252	0.084	146432	0.25
	0.193	0.027	175468	0.32	0.219	0.128	234731	0.34	0.242	0.074	199027	0.24
	0.161	0.029	220828	0.30	0.253	0.121	298468	0.35	0.222	0.067	249675	0.23
	0.177	0.028	266396	0.32	0.235	0.123	362215	0.34	0.224	0.062	299148	0.22
	0.173	0.028	312189	0.31	0.250	0.118	424757	0.35	0.144	0.058	349046	0.20
	0.175	0.028	312189	0.31	0.250	0.117	424757	0.35	0.144	0.055	349046	0.22

[a] OP is optical porosity.
[b] FA is frontal area (m^2).
[c] N/A indicates still air conditions.

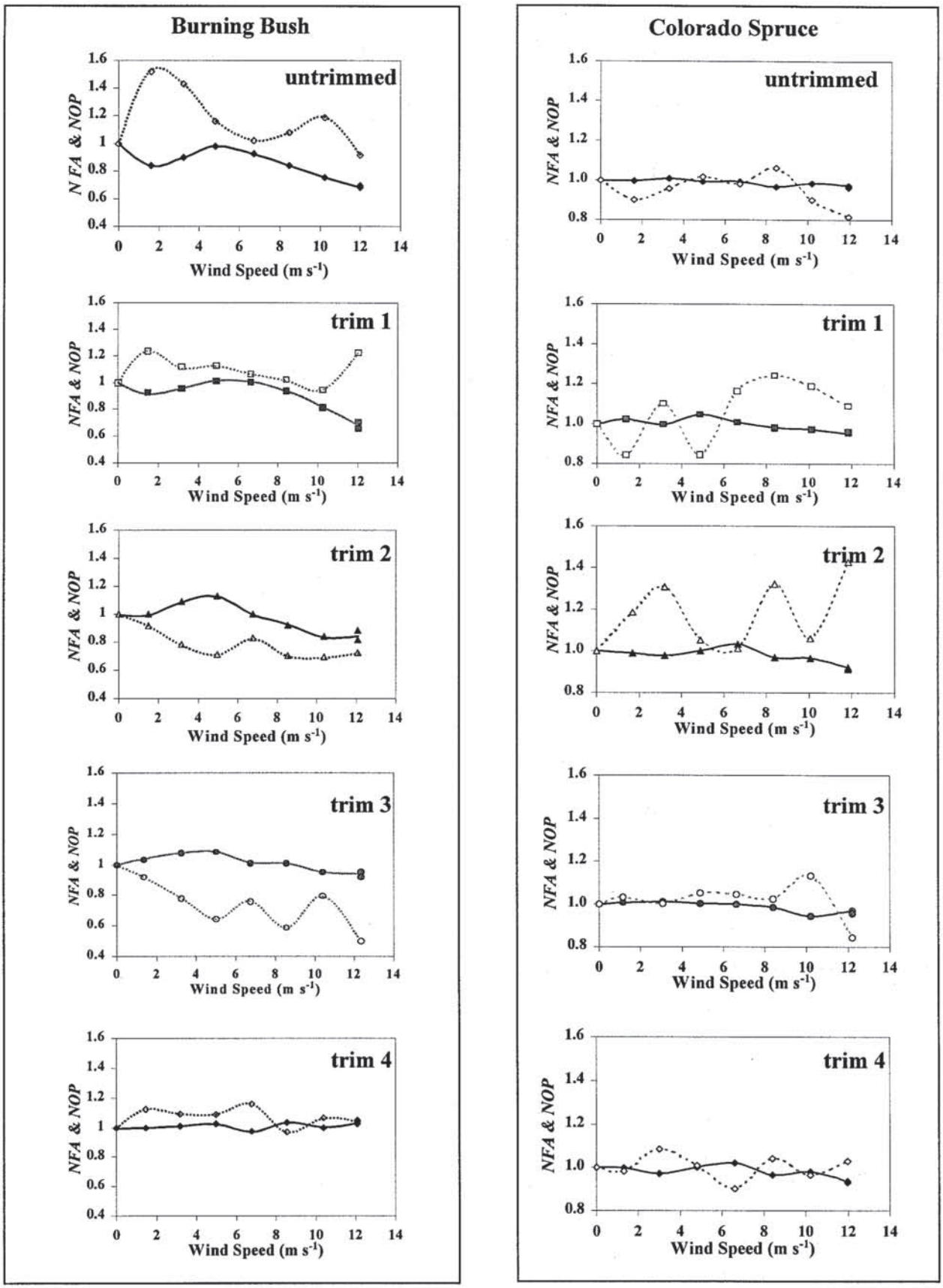
Burning Bush
Colorado Spruce
untrimmed
trim 1
trim 2
trim 3
trim 4
NFA & NOP
Wind Speed (m s-1)

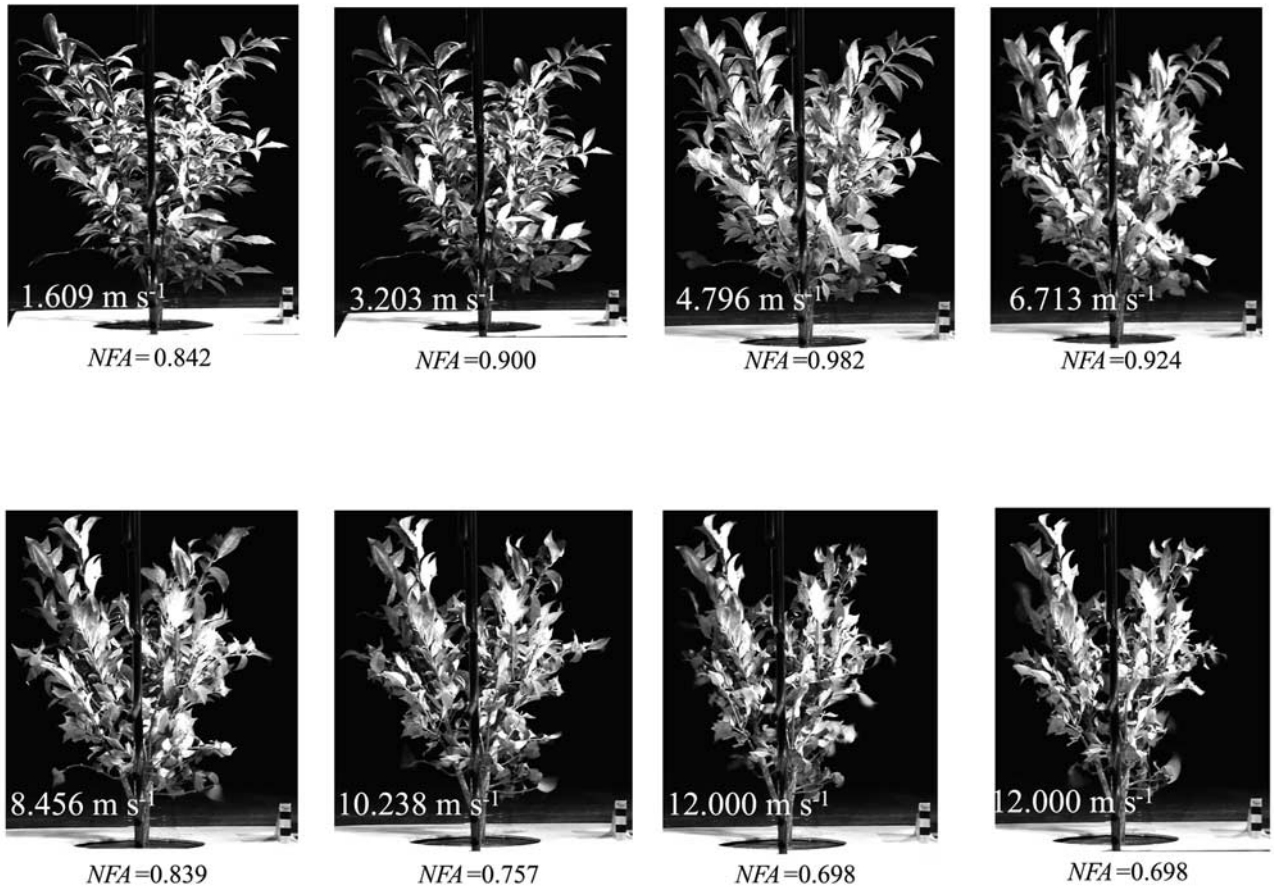

Figure 9. Series of images illustrating the relationship between NFA and wind speed for the Burning Bush. In this case, NFA initially declines from the still air condition then increases to a maximum at a wind speed of $\sim$5 m s^{-1}, thereupon declining to a minimum value at a wind speed of 12 m s^{-1}.

guring in the wind have reported conflicting data regarding the relationship between drag and wind speed. *Mayhead* [1973] analyzed data from *Fraser* [1962] who tested young conifers in a wind tunnel and found that drag increased more nearly with the first rather than the second power of wind speed. Subsequent work by *Roodbarky et al.* [1994], *Gillies et al.* [2000], and the data presented here has not supported this observation. A linear relationship between force and wind speed squared appears to apply to plants with lower flexibility such as the CS and Greasewood tested by *Gillies et al.* [2000]. With increasing plant flexibility it appears the linear relationship does not hold as characterized by the power function relationship observed for the FG (Figure 6).

[27] There is also some indication that the power function relationship between force and wind speed squared observed in the FG also applies to some of the BB data (Table 2). For the BB a power function model fits the data better than the linear model for the untrimmed through the first three trim conditions. By the fourth trim condition (no leaves) the linear model applies equally well as the power model. The BB behaves somewhat like the FG in its first four configurations due to the presence of more leaves and stems, which are themselves more flexible than the main branches and which carry sufficient drag to bend the larger branches more effectively.

4.2. Plant Drag Coefficients

[28] *Taylor* [1988] reported C_d values for a solid cylinder of 0.19 and 0.2 for a solid hemisphere over the R_e range of $5 \times 10^4 - 3 \times 10^5$. *Grant* [1994] measured a C_d of 0.33 (at $R_e = 2.5 \times 10^4$) for a solid cone using a force balance in natural boundary layer winds. The BB broadly resembles an ellipsoid, the CS a cone, and the FG a hemisphere in shape. As found in previous research [e.g., *Wyatt*, 1996; *Grant and Nickling*, 1998; *Gillies et al.*, 2000] the C_d for plants are higher than solid elements of similar form. Above $R_e > 5 \times 10^4$ the average C_d for the BB, CS, and FG in their untrimmed condition are 0.42 ($\pm$0.03), 0.39 ($\pm$0.04), and 0.34 ($\pm$0.06), respectively. The average values of the BB

Figure 8. (opposite) The relationships between normalized frontal area (NFA), normalized optical porosity (NOP), and wind speed for the Burning Bush and Colorado Spruce for each trim condition. NOP is represented by the open symbols and the dashed lines, and NFA is represented by the solid symbols and lines. The continuous lines joining the points are to highlight the pattern of changing NFA and NOP as a function of wind speed.

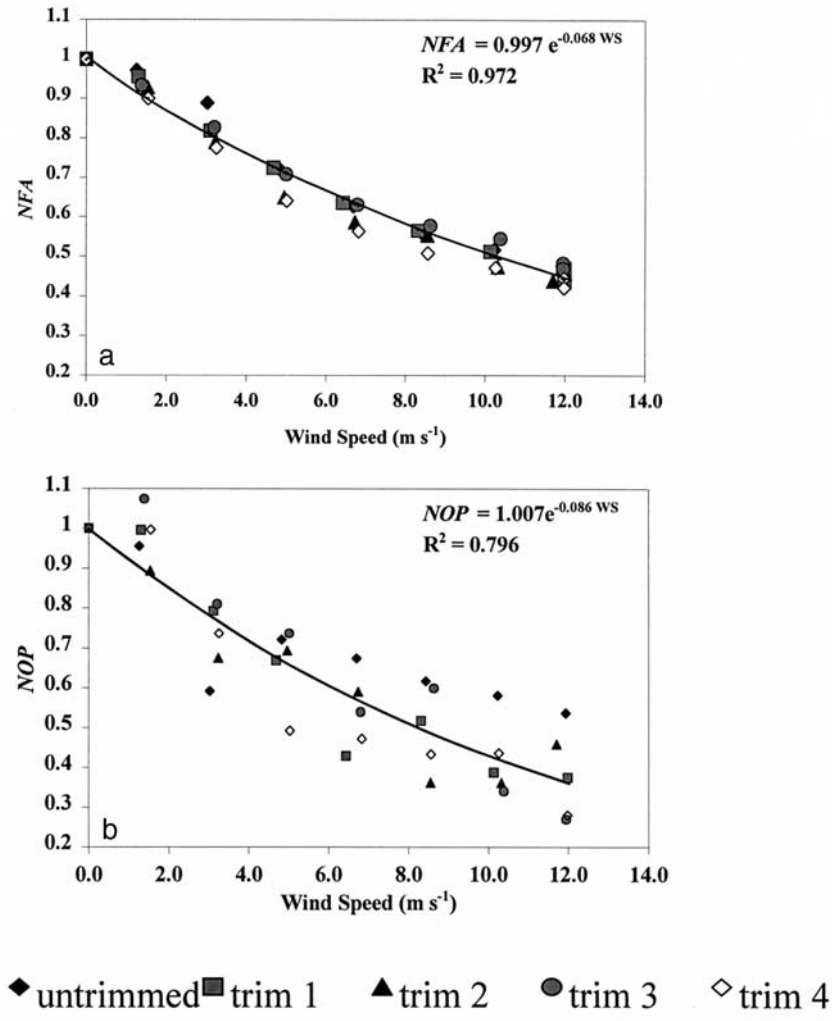

Figure 10. The relationship between (top) normalized frontal area (NFA), (bottom) normalized optical porosity (NOP), and wind speed for the Fountain Grass for each trim condition.

and CS in this R_e range are within measurement uncertainties equivalent. However, because of the more flexible nature of the FG, its C_d was observed to change to a greater degree with R_e than the other two plants.

[29] For the FG the change in FA as a function of wind speed was not in the proportion necessary to result in static C_d values for $R_e > 5 \times 10^4$. For all the trim conditions, including the untrimmed case, the FA did not decrease at fast enough rates with wind speed to maintain a constant C_d for $R_e > 5 \times 10^4$. The relationship between the ratio of FA required to FA measured to maintain a constant C_d with increasing R_e (for $R_e > 5 \times 10^4$) is shown in Figure 13. The FG would have had to decrease its FA by 15% at $R_e \sim 3.5 \times 10^5$ ($\sim$9 m s^{-1}) and 52% at $R_e \sim 1 \times 10^6$ ($\sim$25 m s^{-1}) to maintain a constant C_d, assuming the force was as measured.

[30] While in a state that allows them to easily deform (prior to senescence) grasses in isolated clumps likely affect the partitioning of shear stress between the intervening surface and themselves in a nonlinear fashion. With the decline in C_d as R_e increases following a power function, the momentum absorbing ability of grass clumps declines proportionally as well, meaning a greater percentage of shear stress would be available to act on the intervening surface. If grass complexes were used to control wind erosion or dust emissions, it would be critical to design to a minimum C_d value if erosive winds were expected during the time when plants were in their most flexible state.

[31] For plants that have drag curves similar to the BB and CS that are sparsely distributed, a nonlinear response in the partitioning of shear stress would be expected between $0 < R_e > 2 \times 10^5$. In this situation the plants would absorb increasing amounts of momentum, reaching a peak at some critical wind speed then fall off to a more stable level. The nonlinearity in the lower R_e range is controlled by, in these cases, the physical properties of the BB and CS that allow them to reorient their form to maximize FA (and C_d) at some critical R_e value. After the plant FA maximum is reached it reconfigures in response to the applied drag force, subsequently FA declines, C_d stabilizes, and the ratio of shear stress partitioned between the plants and the intervening surface would become relatively constant. For this pattern to occur the plants would also have to be within a critical range of porosity. As observed for the BB and CS in their highest trimmed states, C_d was relatively invariant with

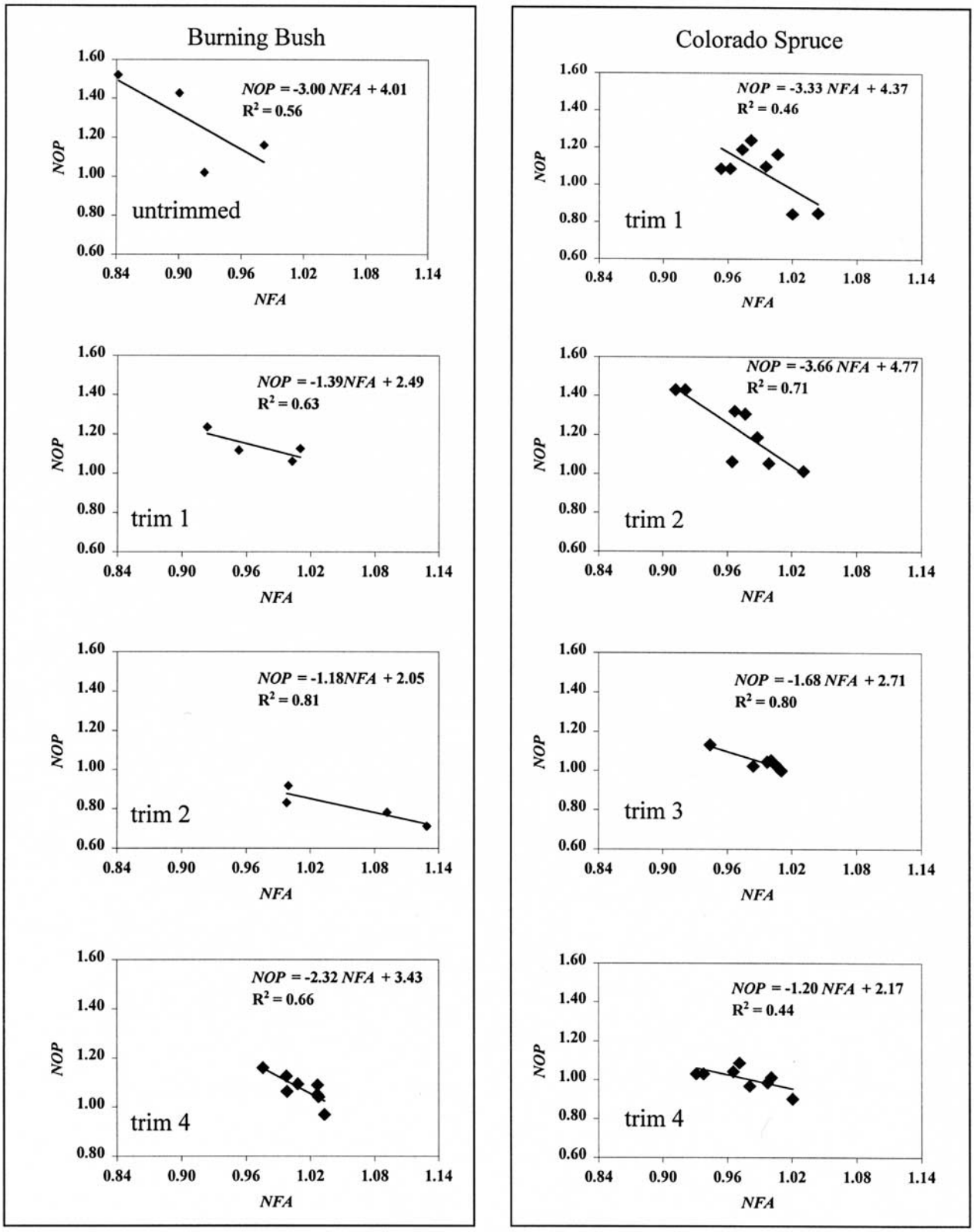

Figure 11. Examples of the relationship between NOP and NFA for the Burning Bush and Colorado Spruce showing the negative correlation between these two parameters. The Burning Bush relationships are for wind speeds <7 m s^{-1}.

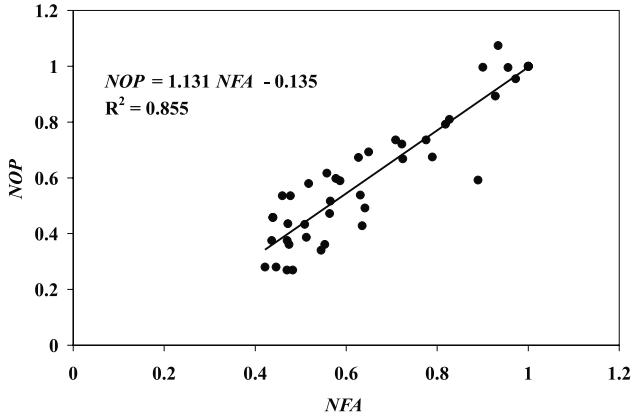

Figure 12. The relationship between normalized frontal area (NFA) and normalized optical porosity (NOP) for the Fountain Grass for each trim condition.

increasing R_e and the plants behaved more like solid elements.

4.3. Porosity and Drag

[32] The effect of porosity on the plant drag coefficients was examined using OP as a surrogate measure for the true three-dimensional porosity structure. For the BB and CS plants their C_d reach a maximum when OP is ~0.19 regardless of trim condition. This is similar to the OP of 0.20 that *Grant and Nickling* [1998] found correlated with the maximum C_d for a porous artificial conifer tree. This suggests that shrubs, or small trees forms, maximize their C_d with OPs of around 0.2. *Grant and Nickling* [1998] offered the explanation that under these conditions the C_d was greater than a solid element form of similar shape due to the wind interaction with multiple bluff bodies along a single flow path. As the BB and CS plants were exposed to higher wind speeds, FAs decreased, OPs generally increased, and more wind could pass through the plants with less of a loss of momentum, which resulted in a lowering of their C_d from a maximum value at a lower R_e. This type of behavior was predicted by *Grant and Nickling* [1998] for flexible porous roughness elements.

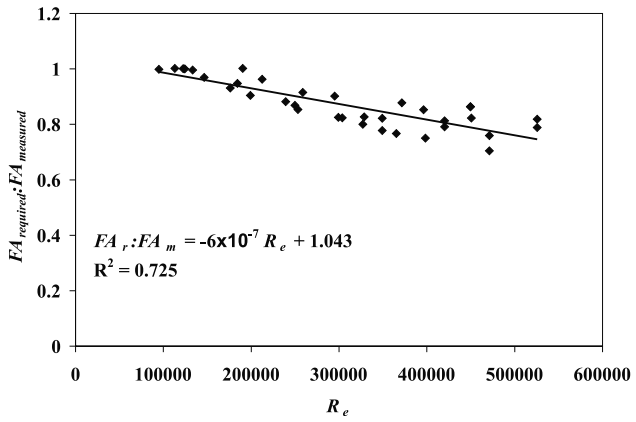

Figure 13. The relationship between the ratio of the frontal area required (FA_r) and frontal area measured (FA_m) to maintain a constant C_d for $R_e > 5 \times 10^4$ for the Fountain Grass, assuming the force was as measured.

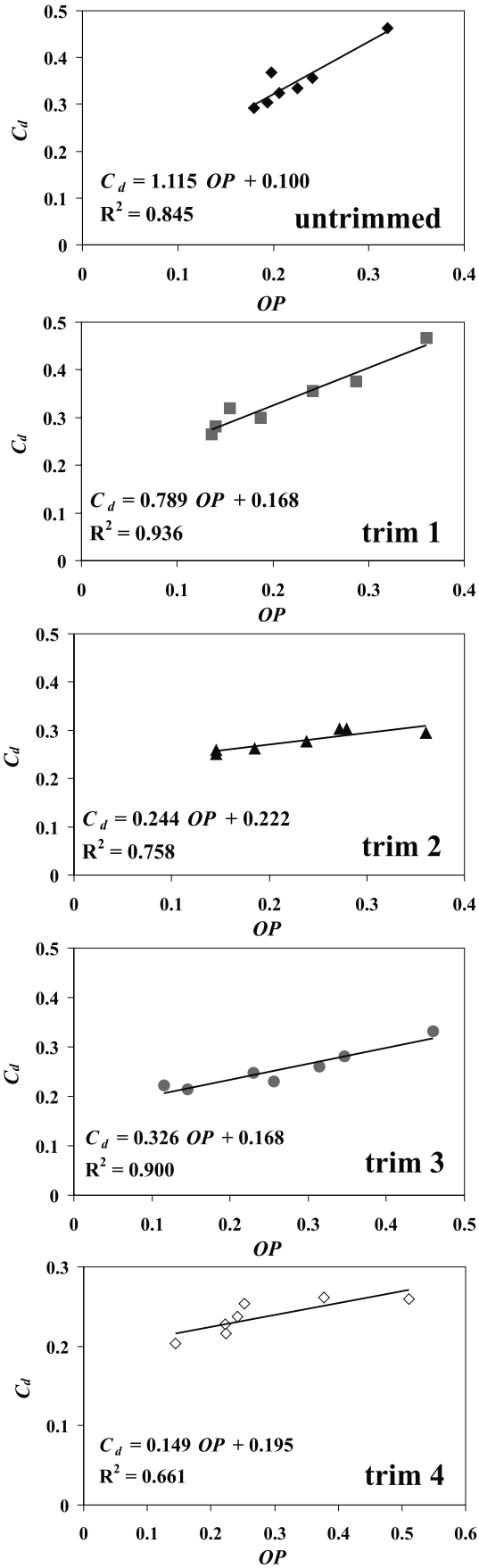

Figure 14. The relationship between OP and C_d for the Fountain Grass for each trim condition.

[33] Unlike the artificial tree of *Grant and Nickling* [1998] and the BB and CS plants in this experiment, the FG does not exhibit any peak in C_d with OP. In all the FG tests C_d was observed to decline linearly with decreasing OP from the initial maximum OP value (Figure 14). The NOP was observed to decrease as an exponential function with wind speed (Figure 10). The FG has a completely different form response than the shrub-type plants. As wind speed (and R_e) increase this plant becomes less porous, but unlike a solid element the C_d remains dependent on R_e to at least 5×10^5. The mechanism responsible for this is the continual deformation or reconfiguration of the grass to a more aerodynamic form.

5. Conclusions

[34] Direct force measurements for three plant species (Burning Bush, Colorado Blue Spruce, and Fountain Grass) placed in a wind tunnel were obtained with a force balance. The force versus wind speed data were used to estimate the isolated C_d for five different porosity configurations for each of the three plants. The C_d for the plants were higher than for similarly shaped solid elements. The drag curves for the BB and CS typically showed an initial increase of C_d with increasing R_e that reached a maximum then subsequently declined with increasing R_e until they became essentially independent of R_e at values $>2 \times 10^5$. The greater the initial still air OP of the BB and CS plants the more quickly their C_d reach independence from R_e. The FG C_d, regardless of trim condition or initial OP, showed dependence on R_e at least to the limit they were exposed to ($>5 \times 10^5$).

[35] Two different form responses to reduce drag with increasing wind speed were observed in the plants tested. The BB and CS plants decreased their FA with increasing wind speed, while at the same time opening their porosity allowing more flow through the plant without a loss of momentum. For small shrub or bush-like forms, maximum C_d appear to correlate with an OP around 0.20. For grass-like forms, in this case the FG, the response to higher wind speeds causes a simultaneous decrease in FA and OP. For drag to be reduced as this mechanistic response occurs, the FG must reconfigure to a more aerodynamic form, which was evidenced by its ever decreasing C_d as a function of R_e, regardless of its trim condition and original still air OP value.

[36] It was observed in this experiment that measuring FA, a much simpler and more easily obtained measure of plant form than OP, provided better information than OP to identify how the plants were responding to increasing wind speeds and how that response was affecting the plant's C_d. This suggests that measurement of plant FA provides a simple means to relate plant form to its aerodynamic characteristics and can be useful to assess the effect of plant aerodynamics on boundary layer flow and fluxes of mass and scalar quantities with the atmosphere.

Notation

A_t element frontal area, m^2.
C_d element drag coefficient, dimensionless.
F total force on a roughness element, N.
FA plant frontal area, m^2.
h plant height, m.
NFA frontal area normalized to still air frontal area value.
NOP optical porosity normalized to still air optical porosity value.
OP optical porosity.
R_e flow Reynolds number, dimensionless.
u_z wind speed at height z, m s^{-1}.
ν kinematic viscosity, m^2 s^{-1}.
ρ air density, kg m^{-3}.

[37] **Acknowledgments.** This material is based, in part, upon work supported by the Cooperative State Research, Education, and Extension Service, U.S. Department of Agriculture, under Agreement 00-35101-9310. Any opinions, findings, conclusion or recommendations expressed in this publication are those of the authors and do not necessarily reflect the view of the U.S. Department of Agriculture. Partial support from the Natural Sciences and Engineering Research Council of Canada to W.G. Nickling is also gratefully acknowledged. We would also like to thank Marco Burlo for helping with the wind tunnel testing and image preparation.

References

Ennos, A. R., The aerodynamics and hydrodynamics of plants, *J. Exp. Biol.*, *202*, 3281–3284, 1999.

Fraser, A. I., Wind tunnel studies of forces acting on the crowns of small trees, in *Report on Forest Research for the Year Ended March, 1962*, report, pp. 178–183, Her Majesty's Stationary Off., London, 1962.

Gillies, J. A., N. Lancaster, W. G. Nickling, and D. Crawley, Field determination of drag forces and shear stress partitioning effects for a desert shrub (*Sarcobatus vermiculatus*, Greasewood), *J. Geophys. Res.*, *105*(D20), 24,871–24,880, 2000.

Grant, P. F., Wind interaction with 3-dimensional porous roughness elements in a natural boundary layer: Empirical observations and theoretical considerations, M. S. thesis, Univ. of Guelph, Ont., Canada, 1994.

Grant, P. F., and W. G. Nickling, Direct field measurement of wind drag on vegetation for application to windbreak design and modelling, *Land Degrad. Dev.*, *9*, 57–66, 1998.

Massman, W. J., and J. C. Weil, An analytical one-dimensional second order closure model of turbulence statistics and the Lagrangian time scale within and above plant canopies of arbitrary structure, *Boundary Layer Meteorol.*, *91*, 81–107, 1999.

Mayhead, G. J., Some drag coefficients for British trees derived from wind tunnel studies, *Agric. Meteorol.*, *12*, 123–130, 1973.

Middleton, G. V. and J. B. Southard, *Mechanics of Sediment Movement*, 401 pp., Soc. for Sediment. Geol., Tulsa, Okla., 1984.

Raupach, M. R., A Lagrangian analysis of scalar transfer in vegetation canopies, *Q. J. R. Meteorol. Soc.*, *113*, 107–120, 1987.

Raupach, M. R., Drag and drag partition on rough surfaces, *Boundary Layer Meteorol.*, *60*, 375–395, 1992.

Roodbarky, H. J., C. J. Baker, A. R. Dawson, and C. J. Wright, Experimental observations of the aerodynamic characteristics of urban trees, *J. Wind Eng. Ind. Aerodyn.*, *52*(1–3), 171–184, 1994.

Taylor, P. A., Turbulent wakes in the atmospheric boundary layer, in *Flow and Transport in the Natural Environment: Advances and Applications*, pp. 270–292, Springer-Verlag, New York, 1988.

Wolfe, S. A., and W. G. Nickling, Shear stress partitioning in sparsely vegetated desert canopies, *Earth Surf. Processes Landforms*, *21*, 607–620, 1996.

Wyatt, V. E., Direct measurement of shear stress partitioning, M. S. thesis, Univ. of Guelph, Guelph, Ont., Canada, 1996.

Wyatt, V. E., and W. G. Nickling, Drag and shear stress partitioning in sparse desert creosote communities, *Can. J. Earth Sci.*, *34*, 1486–1498, 1997.

J. A. Gillies, Division of Atmospheric Sciences, Desert Research Institute, Reno, Nevada, USA 89512. (jackg@dri.edu)

J. King, and W. G. Nickling, Department of Geography, University of Guelph, Guelph, Ontario, Canada N1G 2W1. (nickling@uoguelph.ca; jamesstephenking@hotmail.com)